

value.

⁴L. W. Bruch and I. J. McGee, *J. Chem. Phys.* **52**, 5884 (1970).

⁵W. D. Davison, *Proc. Phys. Soc., London* **87**, 133 (1966).

⁶The χ^2 sum is defined by

$$\chi^2 = \sum_{i=1}^N \frac{[Q_{\text{eff}}^m(v_{1i}) - Q_{\text{eff}}^{\text{th}}(v_{1i})]^2}{[\Delta Q_{\text{eff}}(v_{1i})]^2},$$

where $Q_{\text{eff}}^m(v_{1i})$ are the measured points, $\Delta Q_{\text{eff}}(v_{1i})$ are the errors of the measured points, and $Q_{\text{eff}}^{\text{th}}(v_{1i})$ are the calculated values.

⁷We observed that each potential which gives a good fit to the $\text{He}^4\text{-He}^4$ measurements led, within 0.5%, to the same absolute cross section, which was well within the constraints on the absolute values of the measure-

ments but not in the middle of the region. We have found it impossible to change the potential in such a manner that the calculated cross-section curve can be shifted to lie in the middle of the region of uncertainty and preserve the relative shape. Consequently, the measured points shown in Fig. 2 are shifted by the amount stated in the text to fit the theoretical curves.

⁸H. A. Bethe and E. E. Salpeter, in *Handbuch der Physik*, edited by S. Flügge (Springer, Berlin, 1957), Vol. 35, Part 1, p. 252; M. H. Mittleman, *Phys. Rev.* **188**, 221 (1969).

P. Bertoncini and A. C. Wahl, *Phys. Rev. Lett.* **25**, 991 (1970); H. F. Schaefer, D. R. McLaughlin, F. E. Harris, and B. J. Alder, *Phys. Rev. Lett.* **25**, 988 (1970).

¹⁰A. Fröman, *J. Chem. Phys.* **36**, 1490 (1962).

Observation of Resonance Raman Scattering below the Dissociation Limit in I_2 Vapor*

D. G. Fouche† and R. K. Chang

Department of Engineering and Applied Science, Yale University, New Haven, Connecticut 06520

(Received 13 June 1972)

Inelastic photon scattering from I_2 vapor was observed to change from resonance Raman scattering to resonance fluorescence as a single-mode argon laser was tuned through the 5145-Å gain profile. 3 orders of magnitude enhancement in the Stokes and the first-overtone intensities were measured in going from resonance Raman scattering to resonance fluorescence. The intensity distribution of the first 47 overtones is shown for the laser frequency coincident with the $43 \rightarrow 0 P(12)$ and $43 \rightarrow 0 R(14)$ transitions of $B^3\Pi_{0u^+} \rightarrow X^1\Sigma_{0g^+}$. The resonance Raman cross section of I_2 compared with N_2 was found to be 2.6×10^6 .

The fortunate coincidence of the 5145-Å argon-laser emission with several optical transitions of I_2 vapor¹ [$43 \rightarrow 0 P(12)$ and $43 \rightarrow 0 R(14)$ of $B^3\Pi_{0u^+} \rightarrow X^1\Sigma_{0g^+}$] has stimulated investigations in the resonance fluorescence (RF) by using single-mode laser excitation, tunable over the 5145-Å Doppler gain profile.^{2,3} Studies of RF of I_2 vapor have also been carried out by using multimode lasers^{1,4,5} that have photon energies below the I_2 dissociation limit. However, resonance Raman scattering (RRS) from I_2 has been observed⁶⁻⁸ only when the laser photon energies are above the I_2 dissociation limit. Excitation into the absorption continuum complicates RRS theories,⁹⁻¹¹ as one needs to include both discrete and continuum states. In this Letter, we report the first observation of RRS in a gas below its dissociation limit.

Inelastic photon scattering from I_2 vapor was observed to change from RRS to RF as the single-mode argon-laser frequency was tuned through the 5145-Å gain profile. Associated with this change from RRS to RF, the scattered intensity

of the Stokes line and the first overtone was enhanced by 3 orders of magnitude. The cross section of I_2 in the resonance Raman case is found to be over 6 orders of magnitude larger than the Raman cross section of N_2 gas. Also associated with the transition from RRS to RF, the spectrum of the scattered radiation was observed to be markedly different.

The transitions⁶ from ordinary Raman scattering (ORS) to RRS, then to RF, and finally back to RRS when the incident photon energy is above the continuum limit, are of basic theoretical interest in solids,¹² liquids,¹³ and gases, as well as of practical significance in the possible use of laser backscattering for remote monitoring of air pollutants.¹⁴ Since a significant amount of I_2 vapor is liberated by marine organisms to the atmosphere at the ocean surface, the presence of I_2 vapor can potentially be used as an indicator of marine bioproductivity.¹⁵ Recently I_2 vapor has been used as a resonance filter for Raman scattering experiments¹⁶ and has been proposed as a

frequency stabilizer of the krypton-ion laser.¹⁷

The study of the I_2 molecule by optical spectroscopy has been extensive.^{1,18-21} The intensities of the vibrational overtones serve as sensitive tests for the Rydberg-Klein-Rees (RKR) potential and the Franck-Condon principle.²² In view of this, we have measured the intensity distributions of the first 47 overtones in the I_2 vapor associated with transitions from $V' = 43$ to $V'' = n$ ($n = 1$ to 47) of $B^3\Pi_{ou}^+ \rightarrow X^1\Sigma_{og}^+$, by tuning the single-mode laser within the absorption lines of $43 \rightarrow 0 P(12)$ and $43 \rightarrow 0 R(14)$. Previous workers⁵ used a 5145-Å multimode argon laser, and the intensity distribution of only the first 15 overtones was given.

The experimental arrangement consists of the conventional 90° scattering geometry, Spex double monochromator, RCA GaAs photomultiplier C31034, and photon-counting electronics. A 300-mW multimode argon laser was converted to a tunable single-mode laser by placing a tiltable etalon into the cavity²³ and mounting the front mirror on a piezoelectric translator. The single mode was monitored by an optical spectrum analyzer. The air within the I_2 optical cell was evacuated to less than 1 mTorr, while the I_2 vapor pressure at room temperature is about 250 mTorr.

The changes in the scattered intensity of the Stokes line ($\Delta\nu = 213 \text{ cm}^{-1}$) as the single-mode laser frequency was tuned through the 5145-Å Doppler gain profile are shown in Fig. 1. Qualitatively, this curve is similar to that reported by Kroll and Swanson³ for the second Stokes line. Our results extend over much larger intensity range and are corrected for the incident beam's attenuation through the I_2 cell. The larger intensity peak in Fig. 1 denoted by A coincides with the absorption maximum associated with electronic transitions from $43 \rightarrow 0 P(12)$ and $43 \rightarrow 0 R(14)$ of $B^3\Pi_{ou}^+ \rightarrow X^1\Sigma_{og}^+$. The smaller peak denoted by C coincides with a much weaker absorption associated with the $45 \rightarrow 0 P(64)$ transition.⁵

The distinction between RRS and RF can be made by observing the quenching effect of foreign gas on the scattered intensity.⁶ Since RF involves real transitions, the scattered intensity should decrease inversely as the linewidth of the states, and thus with foreign gas pressure, which causes more collisions. RRS involves virtual transitions to nearly resonant states and thus is not affected by the collision-broadened linewidth. With this in mind, the quenching effect of air on the I_2 emission was investigated at points A and B of

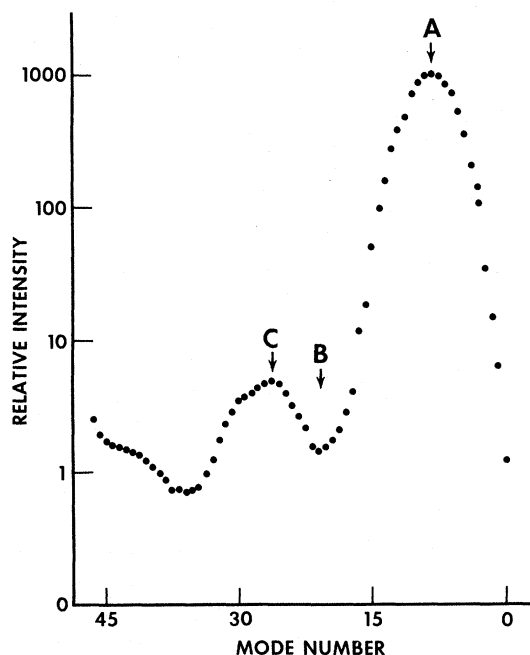


FIG. 1. The relative intensity of the fundamental Stokes band ($\Delta\nu = 213 \text{ cm}^{-1}$) as a function of laser frequency. The vertical axis is the total phototube signal minus the dark current with the spectrometer slits equal to 34 cm^{-1} . Absorption correction has been made for the laser light but not for the scattered light. The horizontal axis is the mode number within the 5145-Å argon-laser Doppler profile. The mode separation is about 115 MHz. Both short- and long-term drifting of the mode makes accurate frequency determination impossible and causes some distortion of the line shape of the above curve.

Fig. 1, and the difference was striking. Pronounced quenching of the scattered intensity was observed at point A. The quenching of the Stokes intensity followed the Stern and Volmer²⁴ equation with 1.8 Torr^{-1} as the apparent quenching constant for air on I_2 , which is at its room-temperature vapor pressure. Because of the observed quenching, we label the scattered radiation at point A as resonance fluorescence. In contrast, at point B virtually no quenching of the scattered intensity was observed. This result led us to label the scattered radiation at point B as resonance Raman scattering.

According to Holzer, Murphy, and Bernstein,⁶ the depolarization ratios of RF and of RRS should be different. In particular, the scattered radiation for RF should be depolarized, whereas for RRS polarized radiation is expected. We found that at both points A and B the scattered radiation was depolarized ($\rho \approx 0.8$). This observation is not inconsistent with the previous assignment

of point *B* as RRS. At point *B* the laser photon energy is only a few gigahertz away from the $V' = 43, J' = 11$ and $V' = 43, J' = 15$ levels. From the uncertainty principle, the lifetime of these virtual transitions is on the order of 10^{-9} sec, while the rotational time is of order 10^{-11} sec. Under such nearly resonant conditions, I_2 can undergo many rotations, as in the RF case, before re-emitting. Thus, RRS can be depolarized if the incident photon energy is very nearly resonant. The condition that RRS be polarized⁶ is true only when the virtual-transition lifetime is short compared to the molecular rotational time. Above the dissociation limit, the Stokes line and first overtone of RRS had ρ much less than 0.8.^{6,8} In the absorption continuum, the intermediate state involved a continuum of states, causing the re-emission time to be much shorter than the rotational time.

The line shapes of the scattered spectra when excited at points *A* and *B* of Fig. 1 were observed by us to be different in two ways. First, excitation at point *A* causes the scattered spectrum to contain a series of small, broad bumps (see Fig. 4 of Ref. 15), which can be attributed to the excited I_2 molecule having undergone a series of inelastic collisions with other I_2 molecules prior to reradiation. The wave-number separation of these bumps is that of the vibrational spacing in the excited state. At point *B*, these bumps disappear. This is reasonable, since for RRS scattering, the virtual-transition lifetime is short compared to the collision time of I_2 molecules at 250 mTorr. Second, the individual line shapes of the overtones differ for excitation at points *A* and *B*. The two transitions $43 \rightarrow 0 P(12)$ and $43 \rightarrow 0 R(14)$ in the neighborhood of point *A* give rise to two fluorescence doublets, which overlap to form a triplet.³ With increasing overtone order, the triplet spreads out because the individual doublet separation increases as $\Delta\nu = (4J' + 2)[B_e'' + \alpha_e''(V'' + \frac{1}{2})]$ with $J' \approx 15$. At point *B*, in addition to the two doublets, another doublet which arises from a transition at point *C* [$45 \rightarrow 0 P(64)$] is added. This doublet spreads out much faster than the previously mentioned doublets, because of its large $J' \approx 63$.

Zare²² has noted that the intensity distributions of the overtones serve as sensitive tests for the RKR potential and Franck-Condon overlap integrals, especially for lines with $V'' \geq 10$. For high vibrational levels in the upper and lower electronic states, the wave functions are rapidly varying oscillatory functions, and thus the overlap inte-

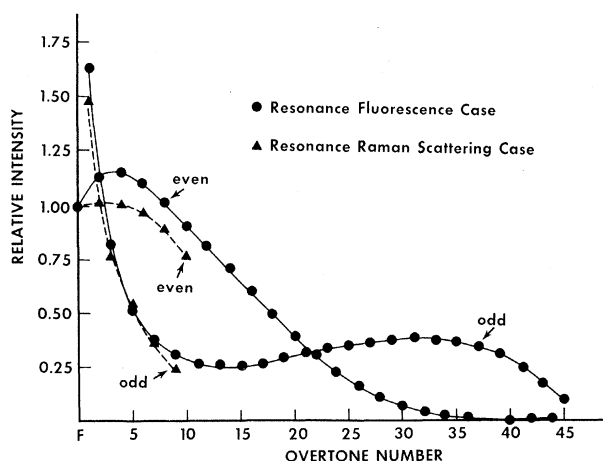


FIG. 2. The relative intensities of the overtones measured with 34-cm^{-1} spectrometer slits. No correction has been made for the self-absorption of scattered radiation through a 5-mm path length of I_2 at 250 mTorr. The absorption coefficients for the fundamental and first five overtones yield (Ref. 5) corrections varying between 1% and 13%. The lines connect the even overtones together and the odd overtones together. The 38th overtone was missing (<0.001). The 47th was observed, but its relative intensity could not be determined accurately. The solid triangles were measured when the laser was at point *B*, while the solid circles were measured when the laser was tuned to point *A* of Fig. 1.

grals depend critically on the phase relation of the initial and final wave functions. Displacement error of only $\pm 0.002 \text{ \AA}$ in the potential minimum can cause gross changes in the intensity distribution. We have measured the intensity distribution up to the 47th overtone when the laser is tuned to point *A*. In Fig. 2, one notes that the intensities of the even and odd overtones alternate. Our results agree well with those of Kurzel and Steinfeld,⁵ who used a multimode laser to observe the first five overtones. Using a multimode excitation, the scattered radiation is mainly due to RF (see Fig. 1). Also shown in Fig. 2 is the intensity distribution for RRS (laser tuned to point *B* of Fig. 1). Beyond $V'' = 10$, the overtone linewidth became comparable to our spectrometer slit width (34 cm^{-1}). Previous works using photographic plates and nonlaser excitation are quoted in Zare²² for $V' = 26$ to $V'' = n$ ($n = 0$ to 39).

The possibility of using laser Raman backscattering for remote detection of air pollutants has stimulated interest as to the orders of magnitude of enhancement in the scattering cross section by going from ORS to RRS and RF. We have com-

pared the Raman cross section of gaseous N_2 , which exhibits only ORS at 5145 Å, to the cross section of I_2 vapor ($V=0$ initial state) at the resonance Raman condition (laser tuned to point B of Fig. 1). The ratio of the RRS cross section of I_2 to that of N_2 was measured to be 2.6×10^6 . An enhancement of 10^6 by RRS is encouraging, especially since we have observed that RRS is hardly (less than 2 times) quenched by air. Consequently, resonance enhancement of the scattering cross section of pollutant molecules in the atmosphere is exceedingly worthwhile.

The differential scattering cross section from the initial I_2 state i (defined as zero energy), plus the incident photon ω_1 , through the intermediate state m ($V'=43$), to the final state f , plus the scattered photon ω_s , may be described by a Breit-Wigner formula²⁵:

$$\sigma_s \propto \frac{| \langle i | m \rangle |^2 | \langle m | f \rangle |^2 \Gamma_{\text{rad}}^2}{(E_m - \hbar\omega_1)^2 + \Gamma^2/4}, \quad (1)$$

where $| \langle i | m \rangle |^2$ and $| \langle m | f \rangle |^2$ are Franck-Condon factors. The total width Γ is the sum of collision (Γ_c), quenching (Γ_q), and radiation (Γ_{rad}) widths. At point A of Fig. 1, we have $E_m - \hbar\omega_1 = 0$ and, upon appropriate integration of Eq. (1) over the I_2 Doppler profile, one obtains the Γ^{-1} quenching dependence, leading to the Stern-Volmer equation. At point B of Fig. 1, we have $E_m - \hbar\omega_1 \gg \Gamma/2$, and thus the cross section should not be quenched, as we have observed.

The intensity distribution of the overtones (at point A of Fig. 1) is a relative measure of $| \langle m | f \rangle |^2$ with $f=1$ to 47. The even and odd overtone intensities are expected to alternate as shown in Fig. 2. At point B , even though one is in the RRS case, the overtone distribution is still due to this Franck-Condon factor. In general, RRS can involve a summation (integral for $\hbar\omega_1$ above dissociation limit) over nearby intermediate states $|m\rangle$ in Eq. (1). This will tend to smooth out the overtone distribution.⁶

The large depolarization ratio observed at points A and B of Fig. 1 is consistent with the fact that only two intermediate rotational states should be considered in Eq. (1). The summation or integration over many rotational states (for the general RRS case) will lead to polarized scattered light, as a result of closure. Further elaboration of our experimental results with theory

will be presented in a forthcoming paper.

We wish to thank Arvid Herzenberg for discussions. The NO_2 paper²⁵ we wrote jointly helped to formulate much of the background of this Letter. We also wish to thank Evan Koslow for assistance in the data analysis.

*Work supported by the National Science Foundation under Grant No. GK-31720.

†National Science Foundation Graduate Fellow.

¹J. I. Steinfeld, J. D. Campbell, and N. A. Weiss, *J. Mol. Spectrosc.* **29**, 204 (1969).

²S. Ezekiel and R. Weiss, *Phys. Rev. Lett.* **20**, 91 (1968).

³M. Kroll and D. Swanson, *Chem. Phys. Lett.* **9**, 115 (1971).

⁴W. Holzer, W. F. Murphy, and H. J. Bernstein, *J. Chem. Phys.* **52**, 469 (1970).

⁵R. B. Kurzel and J. I. Steinfeld, *J. Chem. Phys.* **53**, 3293 (1970).

⁶W. Holzer, W. F. Murphy, and H. J. Bernstein, *J. Chem. Phys.* **52**, 399 (1970).

⁷M. Berjot, M. Jacon, and L. Bernard, *Opt. Commun.* **4**, 117 and 246 (1971).

⁸W. Kiefer and H. J. Bernstein, to be published.

⁹J. Behringer, *Z. Phys.* **229**, 209 (1969).

¹⁰O. Sonnich Mortensen, *Chem. Phys. Lett.* **5**, 515 (1970).

¹¹M. Jacon, M. Berjot, and L. Bernard, *C. R. Acad. Sci.* **273**, 595 (1971).

¹²See, for example, B. Bendow and J. L. Birman, *Phys. Rev. B* **1**, 1678 (1970).

¹³See, for example, O. Sonnich Mortensen, *J. Mol. Spectrosc.* **39**, 48 (1971).

¹⁴See, for example, T. Kobayasi and H. Inaba, *Proc. IEEE* **58**, 1568 (1970).

¹⁵NASA Langley Research Center Report No. NASA SP-285, 1971 (unpublished), p. 76.

¹⁶W. L. Peticolas, G. W. Hibler, J. L. Lippert, A. Peterlin, and H. Olf, *Appl. Phys. Lett.* **18**, 87 (1971).

¹⁷T. W. Hänsch, M. D. Levenson, and A. L. Schawlow, *Phys. Rev. Lett.* **26**, 946 (1971).

¹⁸R. D. Verma, *J. Chem. Phys.* **32**, 738 (1960).

¹⁹D. H. Rank and B. S. Rao, *J. Mol. Spectrosc.* **13**, 34 (1964).

²⁰R. B. Kurzel, E. O. Degenkolb, and J. I. Steinfeld, *J. Chem. Phys.* **56**, 1784 (1972). See earlier references therein.

²¹R. S. Mulliken, *J. Chem. Phys.* **55**, 288 (1971).

²²R. N. Zare, *J. Chem. Phys.* **40**, 1934 (1964).

²³M. Mercher, *Appl. Opt.* **8**, 1103 (1969).

²⁴O. Stern and M. Volmer, *Z. Phys.* **20**, 183 (1919).

²⁵D. G. Fouche, A. Herzenberg, and R. K. Chang, to be published.